Journal of Arid Environments 97 (2013) 182–189

Contents lists available at SciVerse ScienceDirect

Journal of Arid Environments

journal homepage: www.elsevier.com/locate/jaridenv

Soil evaporation beneath and between olive trees in a non-Mediterranean climate under two contrasting irrigation regimes

P.I. Figuerola [a,*], M.C. Rousseaux [b], P.S. Searles [b]

[a] Universidad Nacional de Chilecito, 9 de Julio 22, Chilecito, CP 5360 La Rioja, Argentina
[b] CRILAR-CONICET, Entre Ríos y Mendoza s/n, Anillaco, 5301 La Rioja, Argentina

ARTICLE INFO

Article history:
Received 2 March 2012
Received in revised form
7 March 2013
Accepted 5 July 2013
Available online 20 July 2013

Keywords:
Evett's model
Microadvection
Microlysimeters
Northwest Argentina
Olive

ABSTRACT

Olive production with microirrigation systems has increased in the last 15 years in northwestern Argentina. An irrigation experiment in a commercial olive orchard was conducted from September 2005 to May 2007 under two different irrigation regimes (moderate irrigation MI, and high irrigation HI). From May 2006 to March 2007, soil evaporation was studied using microlysimeters located beneath olive trees, and spatial variability in a sunlit exposed area, and a shaded site was analyzed. The soil evaporation observed under the HI regime was higher than the equilibrium evaporation during the entire experimental period, while the soil evaporation under the MI regime was higher than the equilibrium evaporation only during end of autumn and winter. The high values of evaporation were associated with microadvection in the shaded area, but not in the sunlit sites between olive trees, based on the use of a microadvection coefficient. A model that takes into account the surface energy balance was used to estimate soil evaporation under the olive tree canopy. The first day after irrigation the model underestimated the observed values due to microadvection in the areas wetted by the drip emitters, whereas subsequent days (>1 day) the effect of microadvection was not present.

1. Introduction

Olive production in semi-arid and arid lands have increased during the last 15–20 years in Argentina (from 30,000 to 100,000 ha) which emerged as the largest producer outside of Mediterranean Basin and the Middle East. Most of the new plantations are located in northwest Argentina, a subtropical arid region near the Andes Mountains with climatic characteristics different from those in the Mediterranean. Precipitation events occur primarily in the summer as brief, torrential downpours with almost no winter precipitation. Additionally, both temperatures and crop evapotranspiration are greater than that of the Mediterranean Basin during most of the year (Ayerza and Sibbett, 2001; Gómez Del Campo et al., 2010). Due to the low precipitation in the region, groundwater is the only feasible way to supply adequate water to the crops.

Olive orchards in regions with little natural precipitation in winter will require water application prior to flowering otherwise production falls due to increased flower and fruit drop (Kailis and Harris, 2007), so irrigation must continue to maximize fruit size. In the Mediterranean climate, winter precipitation is sufficient for the olive orchards and irrigation is usually suspended, while in our region irrigation should be applied during these months (Rousseaux et al., 2009).

Soil evaporation can be a significant water loss in high-frequency microirrigation systems. The amount of soil water lost to the atmosphere via soil evaporation from beneath the crop canopy is highly variable, and is influenced by the interaction of potential evaporation, canopy cover and soil water content throughout the growing season. Bonachella et al. (2001) found that the evaporation from the soil wetted by drip emitters represented 4–43% of seasonal orchard evapotranspiration depending on ground cover (36–5%) in drip-irrigated olive orchards in southern Spain. Such drip irrigation systems, coupled with access to deep groundwater resources, are common in large-scale olive orchards in Northwest Argentina. Efforts to minimize water loss by soil evaporation result in more water for plant transpiration and contribute to greater water use efficiency and crop productivity (Cooper and Gregory, 1987; Perry et al., 2009; Tennant and Hall, 2001).

Estimation of soil evaporation (E_s) either beneath the canopy of a growing crop or from bare ground can be performed using microlysimeters (Diaz-Espejo et al., 2005; Eastham and Gregory, 2000; Eastham et al., 1999). Complementary methods for

* Corresponding author. Tel./fax: +54 3825422195.
E-mail addresses: pfiguerola@undec.edu.ar, patfig92@hotmail.com (P.I. Figuerola).

0140-1963/$ – see front matter © 2013 Elsevier Ltd. All rights reserved.
http://dx.doi.org/10.1016/j.jaridenv.2013.07.002

estimating E_s using either empirical (Cooper et al., 1983), semi analytical (Ritchie, 1972) or modeling approaches (Lascano et al., 1987) have also been adopted because microlysimeters are labor-intensive and measuring E_s with microlysimeters does not provide meaningful records during and immediately after precipitations events. In general terms, the E_s after irrigation (or rainfall) is limited only by the available energy at the soil surface (stage one) until the air-soil interface has dried sufficiently to reduce the soil hydraulic conductivity (Ritchie, 1972). Subsequently, the evaporation is inversely related to the square root of time (stage two). Evaporation from the soil wetted by drip emitters occurs at a high rate because the wetted soil is almost always in stage one due to high frequency of irrigation in our area (2–3 times per week in summer and spring). Additionally, the high percentage area of dry soil surface in drip-irrigated systems can result in microadvection of sensible heat from dry to wet areas that increase E_s during high temperature, and low humidity periods (Orgaz et al., 2006). Bonachela et al. (2001) have described microadvection under various ground cover conditions as a function of incident radiation reaching the soil in drip-irrigated olive orchards. However, little information is available about evaporation in non-Mediterranean climates, and how different drip-irrigation regimes can lead to the occurrence of microadvection.

In the present study, soil evaporation rates within olive tree rows receiving two contrasting irrigation regimes were measured using microlysimeters in a drip-irrigated orchard in northwest Argentina. The objectives were to determine the influence of irrigation level positional variation (i.e, the sun versus shade) beneath the olive canopy, investigate the role of irrigation on microadvection, and assess a balanced energy method (i.e Evett model) for estimating the evaporation to compare the rate of water loss if microadvection conditions are present.

Evett et al. (1994) applied the energy balance for a dry soil, and drying soil to estimate evaporation from bare soil. The model was extended to estimate soil evaporation beneath of olive canopy, and air resistances to heat flow near the surface were adjusted.

2. Materials and methods

2.1. Experimental site and irrigation regimes

An irrigation experiment was conducted in a commercial orchard from September 6, 2005 to May 22, 2007 using 6 years-old olive trees (*Olea europaea* L. cv. 'Manzanilla fina'). The orchard is located 15 km east of Aimogasta in the province of La Rioja, Argentina (28°33′S, 66°49′W, 800 m above sea level). The soil was loamy sand with 13% gravel content, had a depth of about 1.5 m, and was classified as an entisol (*torripsamment*) using USDA soil nomenclature. The volumetric soil water content at field capacity and at wilting point were estimated to be slightly greater than 0.20 m m^{-3} and 0.09 m m^{-3}, respectively (Correa-Tedesco et al., 2010). Tree spacing was 4 m × 8 m with a north–south row orientation, and a 23% canopy cover. Tree canopy volume was 15 m^3 with a tree height of 3.5 m at the start of the experiment. Irrigation was supplied by eight drip emitters per tree using two drip lines. The drip lines were spaced approximately 1 m apart (i.e., 0.5 m on each side of the tree trunk), and the emitters were installed at 1 m distances along the drip lines. The soil remained without any vegetation cover during the year due to manual weeding, and the plant canopy in the experimental area was not heavily pruned.

Meteorological data during the experimental period was collected from an automated weather station (Davis Instruments, Hayward, CA, USA) located in a large cleared area with bare soil within the commercial orchard, and was used to calculate daily potential evapotranspiration (ET_o) values with the Penman–Monteith equation by adjusting the non-reference values over bare soil to those over grass using Annex 6 of Allen et al. (1998).

Precipitation in Aimogasta is about 100 mm $year^{-1}$. The average maximum and minimum monthly temperatures were 33.2 °C (January) and 3.7 °C (July), respectively, and annual reference evapotranspiration (ET_o) over grass based on Penman–Monteith equation was around 1600 mm $year^{-1}$with the highest values occurring in summer close to 7 mm day^{-1}

Irrigation was scheduled based on the adjusted ET_o values, crop coefficients, percentage ground cover, and effective precipitation (Allen et al., 1998). The two irrigation regimes were: (1) a high irrigation level (HI) with 110% of ET_o and (2) a moderate irrigation (MI) level with 50% of ET_o. The regimes were maintained from beginning of September to the end of May for each growing season with 2–3 weekly irrigation events. During the winter (June–August), both regimes were irrigated approximately every 2 weeks with the same irrigation dose (i.e., 40% of ET_o) based on Rousseaux et al. (2008). The study presented here includes a whole year cycle of detailed soil evaporation measurements in one HI and one MI experimental plot from May 2006 to March 2007 (i.e., fall to late summer). Each plot consisted of 7 consecutive trees within a crop row. Radiation environment, soil evaporation, and soil temperature were also measured within the plots. Longer-term agronomic and physiological aspects of the larger irrigation experiment have been published by Rousseaux et al. (2009), in which they presented transpiration measurements calculated by measuring the flow of main trunk sap using the heat balance method.

2.2. Measurements of transmissivity

Measurements of photosynthetically active radiation transmissivity (I_s/I_o) of the tree canopy to the soil surface were conducted using a 1-m long, integrated light bar (Cavadevices, Buenos Aires, Argentina) approximately every 2–3 months between May 2006 and March 2007. I_o and I_s are the radiation values measured above and beneath the olive rows, respectively. The measurements were taken every 20 cm over the entire row width at three different positions along the tree row per irrigation plot integrating morning, midday and evening measurements to obtain daily values.

The canopy in the same row was not homogeneous because there is a space between trees, defined as sunlit area, and just under the trees as shaded soil area (Fig. 1). The shaded area was determined since the projected canopy shape on the horizontal surface at midday, where the transmissivity (I_s/I_o) was minimum, and maximum in the sunlit area. The soil area allocated to a tree within the row was 8.8 m^2. The shaded areas measured in the field, were 4.0 m^2 in MI and 4.2 m^2 in HI.

2.3. Observed soil evaporation

Soil evaporation was evaluated using microlysimeters (ML_s) for periods of one week during the months of May, August and November in 2006, and January and March in 2007. The ML_s used in this study were made of PVC tubes (0.06 m i.d. × 0.15 m long), the tube bottom was beveled and a hand auger coupled to the upper part of the ML was made for easy insertion and removal. The day following an irrigation event, the ML_s were inserted into the soil and removed with the soil inside intact. The soil samples were extracted at 10–20 m of the measurement site in the same row, with similar combination of the various soil moisture and radiation conditions showed in Fig. 1. Then, the bottom of each ML was sealed with a plastic cap, weighed, and installed in the soil to their final location (Fig. 1), so that the surface of the soil in the tube and the surrounding soil surface are at the same elevation. The tubes were also wrapped with a thin plastic sheet to minimize the gap between the ML casing

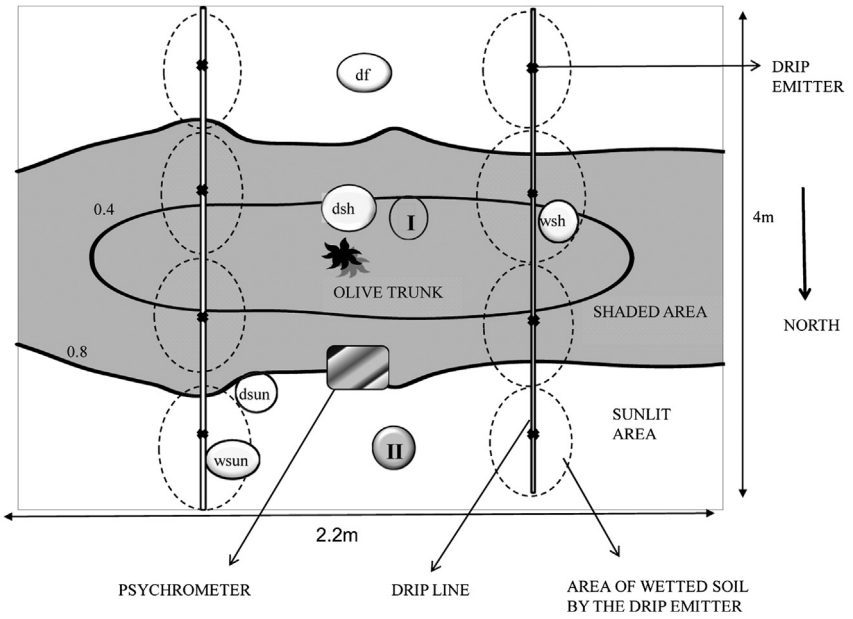

Fig. 1. Schematic representation of the positions of four microlysimeters (white circles) within the tree row for various combinations of soil moisture and radiation conditions at the soil surface (ML_{wsh}, ML_{wsun}, ML_{dsh}, ML_{dsun}). An additional microlysimeter was located equidistant between the two drip lines in the driest area of the tree row, ML_{df}. Two dry soil reference tubes (I and II) and a psychrometer were also present (see Section 2.5 on soil evaporation modeling). Shown in the graph that the shaded area under MI treatment would be limited by photosynthetically active radiation transmissivity (I_s/I_o) ratio of 0.8.

and the surrounding soil. In the subsequent days until the next irrigation, each ML was removed daily from the soil and weighed to calculate soil evaporation from mass loss, and returned to their respective locations. All measurements were performed between 0730 and 0930 h solar time using an electronic balance (model OAC-24, Moretti, Buenos Aires) with a 1 g resolution.

The ML_s location was within the tree row for each irrigation regime (Fig. 1). Five of the ML_s were placed in the combination of soil wetting by the drip emitter and radiation conditions created by the tree canopy. The ML_s in wetted soil were abbreviated as ML_{wsh} (wet-shade) and ML_{wsun} (wet-sun) and those in the drier soil, no wetting, are ML_{dsh} (dry-shade) and ML_{dsun} (dry-sun). The fifth ML in the tree row was located between the two drip lines and equidistant from neighboring tree canopies within the row (ML_{df}) in the driest area of the tree row.

Using the daily measured evaporation from the ML (mm) and the diameters of the soil surface wetted by the emitters, the evaporation from the shaded (E_{sh}) and sunlit (E_{sun}) areas were obtained as:

$$E_{sh} = f_{wsh}ML_{wsh} + (1 - f_{wsh})ML_{dsh} \quad (1)$$

$$E_{sun} = f_{wsun}ML_{wsun} + (1 - f_{wsun})\left(0.5ML_{dsun} + 0.5ML_{df}\right) \quad (2)$$

where f_{wsh} and f_{wsun} are the fraction of wetted soil surface in the sunlit and shaded areas, respectively. Soil evaporation decreases with distance from the emitters (Bonachela et al., 2001). We found that usually evaporation from ML_{df} was less than ML_{dsun}. Similar weight was given to both microlysimeters because they represent roughly similar areas in the sunlit area.

The soil evaporation (E_s) was limited to the area within the tree row, thus, E_s was obtained as:

$$E_s = E_{sh} + E_{sun} \quad (3)$$

The soil evaporation in the inter-row space was negligible most of the year due to lack of precipitation, the E_s of the orchard should include both the fraction of the area designated to the tree row (25%) and the inter-row spacing (75%).

2.4. Microadvection

It is known that latent heat flux from well-watered crops can exceed net radiation, when an excess energy is provided by advection of sensible heat from adjacent dry fields. On a small scale, the spatial heterogeneity in soil water status caused by drip-irrigation may raise E_s due to microadvection of sensible heat from dry to wet soil.

Advection in agricultural systems has been defined as occurring when $E_s/E_{eq} > 1.26$ (Lang et al., 1974) where E_{eq} represents the lower evaporation limit from moist surfaces (Brutsaert, 1982). Diaz-Espejo et al. (2005) found microadvection in sunflower systems when $E_s/E_{eq} > 1.4$.

Bonachela et al. (2001) refers to microadvection in an olive orchard when the soil evaporation in wet zones of drip-irrigation (E_{sw}) is greater than potential soil evaporation (E_{so}), assuming complete and uniform soil wetting. A microadvection coefficient (K_w) was defined as the ratio between E_{sw} and E_{so} (Bonachela et al., 2001). Thus, we calculated E_{so} as:

$$E_{so} = [s/(s+\gamma)]R_N(I_s/I_0) + [\gamma/(s+\gamma)]\Delta e[2.6(1+0.54u)] \quad (4)$$

where E_{so} is the soil evaporation during the energy limiting stage (mm day^{-1}), s is the slope of the vapor pressure curve (kPa $^{\circ}C^{-1}$), γ is the psychrometric constant (kPa $^{\circ}C^{-1}$), R_N is the net radiation (mm day^{-1}), I_s/I_o is the daily PAR (photosynthetically active radiation) transmissivity per each period, Δe is the vapor pressure deficit (mb), and u is the wind speed at 2 m height (m s^{-1}). Eq. (4) is identical to the Penman reference ET equation (Brutsaert, 1982) except for the inclusion of the fraction I_s/I_o in the irradiative term of the equation. Due to the difficulty of obtaining the net radiation reaching the soil beneath the canopy (Mariscal, 1998) this was replaced by the term $R_N(I_s/I_o)$. Bonachela et al. (1999) observed that the net radiation reaching the soil is slightly higher than the PAR

radiation, but they achieved good results using Equation (4) to estimate soil evaporation for the energy-limiting stage under the olive tree.

According to Diaz-Espejo et al. (2005) if there is a situation of advection a temperature inversion ($\gamma < 0$) between soil and air causes a downward sensible heat flux ($H = k_a\gamma$; k_a is the air diffusivity coefficient) at the ground that is converted to latent heat flux (λE_s; λ is the latent evaporation heat), and an advection term of latent flux (λE_a) is added to equilibrium evaporation (λE_{eq}). We evaluated the vertical temperature gradient (γ) near the soil surface using the drying soil temperature (T_s) and air temperature (T_a) at 15 cm in the sunlit and shaded areas for both irrigation regimes. The vertical gradient was defined as $\gamma = -\mathbf{\Delta}T/\mathbf{\Delta}z$, with $\mathbf{\Delta}z = 0.15$ m, and $\mathbf{\Delta}T = (T_a - T_s)$. The gradient magnitude will be somewhat greater than expected because we made use of soil temperature (where the thermocouple was buried superficially) rather than air temperature, but what is significant for this paper is the gradient direction.

2.5. Soil evaporation modeling

Fox (1968), and later Ben-Asher et al. (1983), and Evett et al. (1994) described an E_s prediction method based on subtracting the energy balance equations written for a dry and a drying soil. Because E_s is zero for a dry soil this gives an expression for E_s from the drying soil in terms of the other energy balance terms. The method requires a column of dry soil embedded in the field of drying soil, and measurements of the surface temperatures of the dry soil and of the drying field soil. Evett's model (1994) includes wind speed to parameterize the resistance to heat diffusion on dry soil and soil drying, and assumes that for any diurnal period the integrated soil heat flux and short wave radiation terms are negligible. Daily evaporation was obtained by integrating the model at time intervals of one hour. The model is:

$$\int_{t_1}^{t_2} E_s dt = \varepsilon_s \sigma \int_{t_1}^{t_2} \left(T_d^4 - T_s^4\right) dt + \rho C_p \int_{t_1}^{t_2} [(T_d - T_a)/r_d] dt - \rho C_p \times \int_{t_1}^{t_2} [(T_s - T_a)/r_s] dt \quad (5)$$

where T_d is the dry reference soil temperature, T_s is the drying soil temperature, t_1 and t_2 represent time, ε_s is the soil emissivity, σ is the Stefan–Boltzmann constant, C_p is the specific air heat, ρ is the air density, and r_d and r_s are the air resistances for sensible heat flux of dry and drying soils. This implies a convection condition for a dry soil, and of neutrality for a drying soil. The air resistances were calculated as suggested by Evett et al. (1994):

$$r_d^{-1} = D_{hd} = 0.0038202u^{0.17} \quad (6)$$

$$r_s^{-1} = D_{hs} = k^2 u / \ln^2(z/z_o) \quad (7)$$

where z is the reference height (m), z_o is the roughness length (m) equal to 0.0003 m (Kreith and Sellers, 1975); k is the von Karman constant (0.41), and u is the horizontal wind speed (m s^{-1}) at the reference height. The air resistances were initially derived with the reference wind speed at 2 m, but these were corrected by us to a reference height of 0.2 m using the expression of Cohen (1983) in which the leaf area index determines the reduction of wind speed beneath the canopy. This model has the advantage that the soil resistance does not have to be known but only the air resistance as a function of wind speed.

For each irrigation regime, two reference dry soil samples were packed in PVC tubes with plastic cap at the bottom (0.16 m i.d. and 0.15 m long) and were buried in the sunlit area and in the shaded area under the tree row (Fig. 1), so that the soil surfaces in the tubes were at the same elevation as the field surface. To allow thermal equilibration of the reference soil, the tubes were set a week prior to the experiment and remained in the soil throughout the experimental cycle. They were covered with plastic cap during irrigation and when the measurements were not executed to prevent wetting.

In both cases, the tubes were positioned between the drip lines in drying soil, but away from the soil surface directly wetted by the drip emitters (Fig. 1). The dry reference soil temperature (T_d) and the drying soil (T_s) temperature were measured using two copper-constantan thermocouples. One thermocouple was placed in the PVC tube with the reference dry soil, while the other was positioned just outside the tube. The thermocouples were covered with a 1-mm layer of soil. The soil temperature values were recorded every 15 min by a data logger (Cavadevices, Buenos Aires, Argentina). Air temperature (T_a) and vapor pressure (e) 15 cm above the soil surface were also obtained every 15 min for each irrigation regime using a psychrometer (Figuerola and Berliner, 2006).

3. Results and discussion

3.1. The transmissivity

The spatial distribution of PAR transmissivity (I_s/I_o) changes throughout the year depending on the elevation of the sun, and tree size and shape. The transmittance in the different parts of the ground beneath the tree row does not have the same value throughout the day. The daily integrated value remained almost constant over short periods of the experiment, but changed for fall, spring, summer and winter. This integrated daily value is presented with isolines in Fig. 1 to MI treatment and Fig. 2 to HI treatment in summer.

As would be expected, the daily PAR transmissivity (I_s/I_o) at the soil surface was lowest near the trunk and highest towards the edges of the canopy (Fig. 2). The shape of the tree canopies was

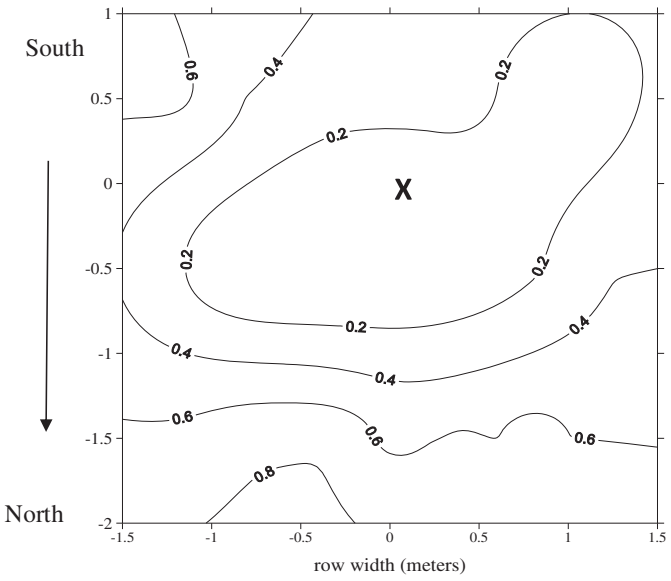

Fig. 2. Distribution of daily photosynthetically active radiation transmissivity (I_s/I_o) beneath and between olive trees within the tree row for the high irrigation regime in summer (January). The tree trunk is shown as an **X**.

asymmetrical due to strong southwest winds with most of the foliage being to the northwest of the tree trunk. Interestingly, daily I_s/I_o was greater under the MI than the HI irrigation regime. This result is likely explained by differences in vegetative growth and leaf abscission between the two regimes. Previous measurements indicated that leaf area density and total leaf area per tree were 20% and 30% less under the MI than under the HI regime (Rousseaux et al., 2009). Thus, more PAR was transmitted to the soil surface under the MI regime.

3.2. Positional effects on soil evaporation

The millimeters evaporated from individual microlysimeters (ML; 0.06 m in diameter) in the wet-sun microenvironments (ML_{wsun}) under the MI and HI irrigation regime were greater than in the wet-shade (ML_{wsh}) for the first day after irrigation in the warm months (i.e., spring and summer) (Table 1) ($p = 0.10$ probability level). In these months the millimeters evaporated from ML_{wsun} and ML_{wsh} under the MI regime were higher than in HI treatment, this may be due to greater radiation reaching the soil (Fig. 2) but the difference was not significant ($p = 0.10$). As expected, a fairly high evaporation was maintained at this time of year until the next irrigation event because irrigation frequency was 2–3 times per week. In the cooler months (autumn winter) the opposite occurred, ML_{wsh} was greater than ML_{wsun} for both irrigation regimes ($p = 0.10$). Under MI treatment on subsequent days after irrigation (>1 day) there was a significant difference ($p = 0.10$) between ML_{wsun} and $ML_{wsh,}$ but under the HI regime the difference was not significant ($p = 0.10$) (Table 1). Our results were consistent with those found by Bonachela et al. (1999) in the warm months, when the highest irradiance under the canopy (ML_{wsh} in MI regime) reaching the soil for the first day after irrigation, evaporation was higher than ML_{wsh} in HI regime, and the opposite occurred for subsequent days after irrigation (>1 day). In all cases, the ML evaporation was much lower in the dry soil than in the wet soil (data not shown).

The evaporation from microlysimeters ML_{wsh} and ML_{wsun} can be estimated from environmental variables, and from the monthly values empirical equations were obtained. The environmental variables that influence the evaporation are mainly the radiation incident on the wet spots and ET_o (Orgaz et al., 2006). We used the PAR transmissivity to assess radiation reaching the wet spot below the canopy from the two irrigation regimes, and then ML_{wsh} resulted:

$$ML_{wsh} = ET_o\left[0.8816\exp(3.8521(I_s/I_o))F_{gc}\right] \quad (8)$$

where F_{gc} is the ground cover fraction, and (I_s/I_o) measured on each spot. The relationship was a r^2 equal to 0.85.

Table 1
Measured daily evaporation from the wet microlysimeters in the shaded area (ML_{wsh}) and sunlit (ML_{wsun}) microenvironments for moderate (MI) and high (HI) irrigation regimes. The values are averaged as warm (November, January, and March) and cool (May, August) months, with the standard error. * Significant differences between ML_{wsun} and ML_{wsh} for the same irrigation regime ($p = 0.10$ probability level), and ** no significant differences ($p = 0.10$).

	Months	MI treatment		HI treatment	
		ML_{wsun} (mm day^{-1})	ML_{wsh} (mm day^{-1})	ML_{wsun} (mm day^{-1})	ML_{wsh} (mm day^{-1})
First day after irrigation	Warm	2.07 ± 0.31	1.55 ± 0.24*	1.77 ± 0.24	1.03 ± 0.27*
	Cool	0.32 ± 0.52	1.39 ± 0.11*	1.14 ± 0.36	2.20 ± 0.51*
Subsequent days after irrigation (>1 day)	Warm	1.38 ± 0.01	0.86 ± 0.23*	1.03 ± 0.34	1.89 ± 0.71**
	Cool	0.44 ± 0.11	1.40 ± 0.73*	0.61 ± 0.24	0.93 ± 0.31**

Evaporation from a circular moist area can be described according to the mass transfer theory (Brutsaert, 1982) assuming that the surface vapor pressure of the wetted area is at saturation. Thus an empirical expression can be obtained to ML_{wsun}:

$$ML_{wsun} = -0.0055(\Delta e)^2 + 0.2492(\Delta e) - 0.4319 \quad (9)$$

where Δe is the vapor pressure deficit close to surface obtained from psychrometer. The maximum observed Δe was in November, and the r^2 value of the relationship was 0.87. Soil evaporation below the canopy (ML_{wsh}) was not closely coupled to seasonal changes in saturation deficit, with r^2 of 0.42. The use of different variables in these two relationships indicates the importance of considering positional effects at the soil surface in olive tree rows.

Finally, soil evaporation (E_s) in the tree row can be evaluated from the shaded (E_{sh}) and sunlit areas (E_{sun}) using Eqs. (1) and (2) respectively. Soil area wetted by the emitters is included in these equations. This area was approximately 50% lower under the MI than under the HI regime throughout the experimental period except for the winter when both regimes were similarly irrigated. In the spring and summer months (November, January, March), E_{sun} was almost always greater than E_{sh} in the tree row under both irrigation regimes due to the high soil evaporation in the space between the trees (Table 2). But, during the autumn and winter (May and August), the results were similar to Table 1, especially under the MI regime where E_{sh} was greater than $E_{sun,}$ with significant difference ($p = 0.10$). The annual water loss by evaporation for HI was 25% higher than for MI treatment.

3.3. Soil evaporation (%)

Evapotranspiration (ET) was determined as the sum of soil evaporation and transpiration measured with sap flow method (Rousseaux et al., 2009). This was used to evaluate the relative importance of seasonal E_s losses represented as a fraction of ET. The evaporation rate for HI and MI treatments (Fig. 3) were not significantly different for the periods considered ($p = 0.10$). The soil evaporation appeared to be higher in the MI regime in January (summer) due to two rainfall events (7 mm) which occurred shortly before the measurement period.

In this orchard with its 23% crop cover, the overall E_s percentage values during the warmer months from November (spring) to March (late summer) indicated that E_s was approximately 27% of orchard ET. In May (autumn), water lost by E_s was 40% of orchard ET due to over-irrigation, while the E_s percentage was still greater in August (winter) due in part to very low transpiration by the tree canopies under cold air temperature conditions (Rousseaux et al., 2009). Testi et al. (2006) determined E_s to be 40% of the annual ET in a typically Mediterranean traditional olive orchard and 35% in an intensive orchard. Our case coincides with these values (36%) but a high percentage of water loss occurred in winter.

Table 2
Measured daily soil evaporation (mm day^{-1}) in sunlit (E_{sun}) and shaded (E_{sh}) areas per month, and microadvective coefficients monthly for the wet-sun (K_{wsun}) and wet-shade (K_{wsh}) areas. Under moderate (MI) and high (HI) irrigation regimes the measurements are as follows.

Months	MI treatment				HI treatment			
	E_{sun}	E_{sh}	K_{wsun}	K_{wsh}	E_{sun}	E_{sh}	K_{wsun}	K_{wsh}
January	1.76	1.02	0.98	1.04	1.47	1.24	1.08	1.22
March	0.67	0.39	0.85	0.85	0.88	1.07	0.93	1.30
May	0.27	0.98	0.64	1.37	0.88	1.02	2.22	1.65
August	0.18	1.00	0.00	1.60	0.40	0.57	0.00	3.00
November	1.05	1.03	0.84	1.14	1.72	1.25	0.97	1.25

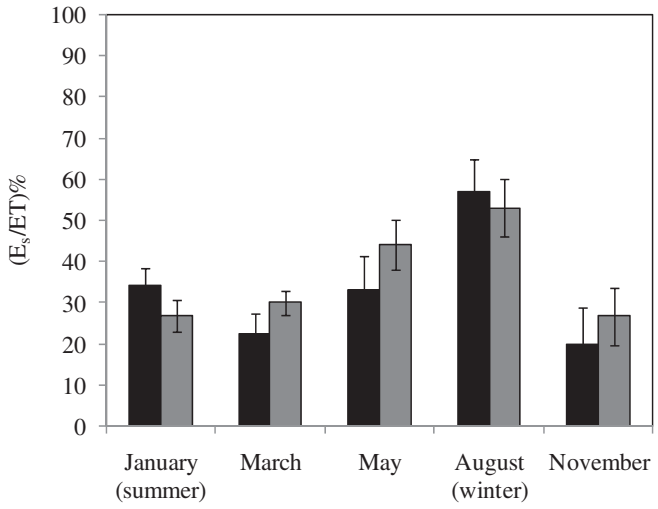

Fig. 3. The ratio of soil evaporation (E_s) to orchard evapotranspiration (ET) shown as a percentage for the moderate (black) and high (gray) irrigation regimes, with standard error respectively.

3.4. Microadvection

The presence of microadvection in this drip-irrigated orchard was evaluated comparing measures E_s with E_{eq} (it is the first term of eq. (4)) for the first day after irrigation (Fig. 4). E_s under the MI regime in the warm months of January, March and November was less than $1.4E_{eq}$, therefore microadvection was not occurring based on the threshold defined by Diaz-Espejo et al. (2005). However E_s was greater than $1.4E_{eq}$ during the cooler months of May and August. Microadvection was observed under the HI regime for all experimental periods since E_s values were greater than $1.26E_{eq}$ and $1.4E_{eq}$, (Diaz-Espejo et al., 2005; Lang et al., 1974). The E_s values under the HI regime in January (mid-summer) were lowest (i.e., near of $1.4E_{eq}$) for two days after a rain event, this reduces the effect of advection as would be expected. On average, we calculated that the second term of Eq. (4) (the advection term) was 20% greater under HI than under MI regime.

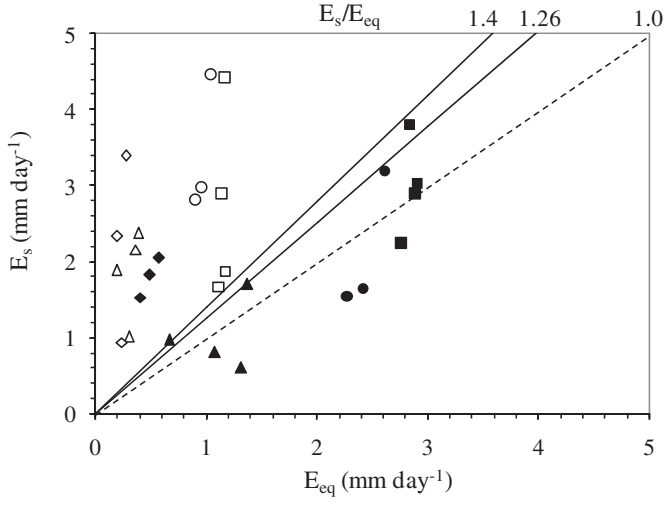

Fig. 4. Relationship between daily values of soil evaporation (E_s) and the equilibrium evaporation (E_{eq}) in a drip-irrigated olive orchard for the first day after irrigation. The symbols are for the months of January: ■ MI and □ HI regime; March: ▲ MI and Δ HI; May–August: ◆ MI and ◇ HI; November: ● MI and ○ HI. The solid lines indicate the proposed ratios of $E_s/E_{eq} = 1.26$ (Lang et al., 1974) and $E_s/E_{eq} = 1.4$ (Diaz-Espejo et al., 2005) above which microadvection may occur.

The microadvection coefficient, K_w, (Bonachela et al., 2001) considers the existence of microadvection when this is greater than one. When separating the wet drip-irrigation area into shaded (K_{wsh}) and sunlit (K_{wsun}) zones, the monthly K_{wsh} values was greater than 1 with the exception of the March value under the MI regime (Table 2). However, the monthly K_{wsun} values are typically lower than 1. Only the May K_{wsun} value (2.22) under the HI regime is greater than 1. Essentially, the microadvection effect is present in the shaded zone of the wet drip-irrigation area. This can explain the greater E_s values found under the wet shade microlysimeters versus the wet sun microlysimeters during the cool months (May, August) in Table 1, and the greater overall E_{sh} values relative to E_{sun} for this same time period in Table 2.

The hourly vertical temperature gradient values (γ) near the soil surface were obtained and are shown for the first day after irrigation under the HI regime in Fig. 5. In November (spring; Fig. 5a), in the shaded area under the tree row microadvection was present since $\gamma_{sh} < 0$ indicating downward sensible heat for the entire 24-h period (with high air temperature, Fig. 5a), while γ_{sun} in the sunlit area between trees within a row is $\gamma_{sun} < 0$ only at night when the soil was cooling. The dynamic of the vertical gradient between rows (i.e., inter-row spacing) was similar to that of the sunlit area

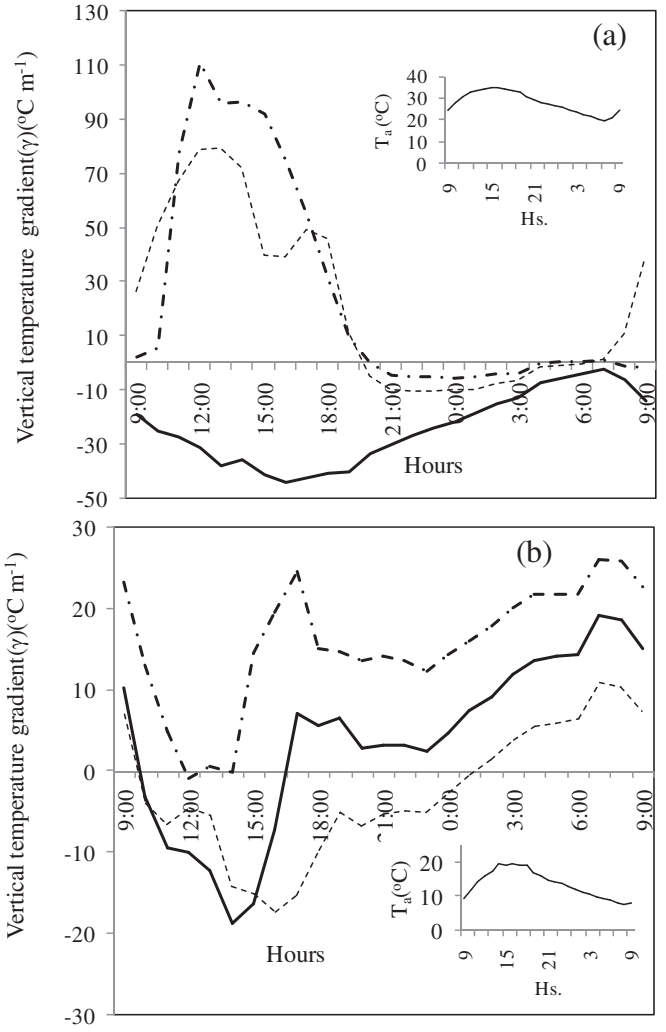

Fig. 5. The average vertical temperature gradient (γ) for the first day after irrigation under the high irrigation regime for the shaded area (—), sunlit area (–), and the inter-row (— - —). November is (a), and May is (b). Air temperature at 10 cm was included in the graph to the corresponding to the month.

between trees in November. In May (fall; Fig. 5b), γ_{sh} and γ_{sun} are both negative during the daylight hours indicating advection, but not at night because soil temperature descended slower than air temperature due to high water soil content (0.24 m m^{-3} in the HI regime). Overall, the vertical temperature gradient results concur with those of the microadvection coefficients (K_w) in Table 2.

As suggested by other authors (Lee et al., 2004; McNaughton and Laubach, 1998), the sensible heat flux might be generated from other sources in addition to horizontal heat advection. The temperature differences between shaded and non-shaded parts of the canopy can generate convective cells (Raupach, 1979), those vertical movements could result in the injection of sensible heat into the canopy (Berliner, 1998; Figuerola and Berliner, 2006). From Fig. 5a, a maximum upward H in the sunlit (γ_{sun}) and inter-row (γ_{irow}) areas occurred at midday in November (spring) and three hours after a maximum downward H at the soil surface of the shaded (γ_{sh}) area occurred. This may indicate that there was sensible heat injected into the canopy from the inter-row that then descended from the canopy to the soil surface. No evidence of such phenomena was apparent for the cooler months (Fig. 5b).

In Fig. 6, a maximum upward sensible heat flux (H) in the inter-row (with $\gamma_{irow} >> 0$) coincided with a maximum downward heat flux in the shaded area ($\gamma_{sh} << 0$) under the HI regime. This further suggests the potential importance of convective activity on the stable condition beneath olive tree canopies in the shaded area, but more testing should be done. The daily γ_{sh} values under MI were less negative ($\gamma_{sh} \sim$ cte < 0) than under the HI regime.

3.5. Evett's model

Evett's model (1994) is based on surface energy balance, and the model (Eq. (5)) is not balanced if excess energy is provided from the advection of sensible heat flux. The estimated monthly E_s values for the first day after irrigation in all periods had a tendency to underestimate the observed E_s, and the root mean square error (RMSE) between observed and calculated measurements was large (0.8 mm day^{-1}). In contrast, the estimated monthly E_s values for subsequent days after irrigation (>1 day) were consistent with the observed values, and the RMSE was lower (0.5 mm day^{-1}).

We also calculated the microadvection coefficient, K_w, for the first day after irrigation and subsequent days and compared them with the RMSE for each period as shown in Fig. 7. The RMSE

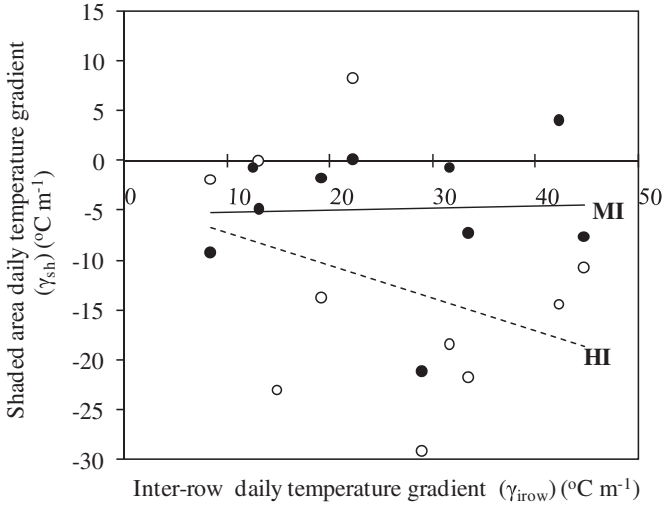

Fig. 6. Daily vertical temperature gradient near the soil surface in the crop inter-row crop (γ_{irow}) versus the gradient in the shaded area (γ_{sh}) under the moderate (MI; ●) and high (HI; ○) irrigation regimes. Best-fit lines are also shown.

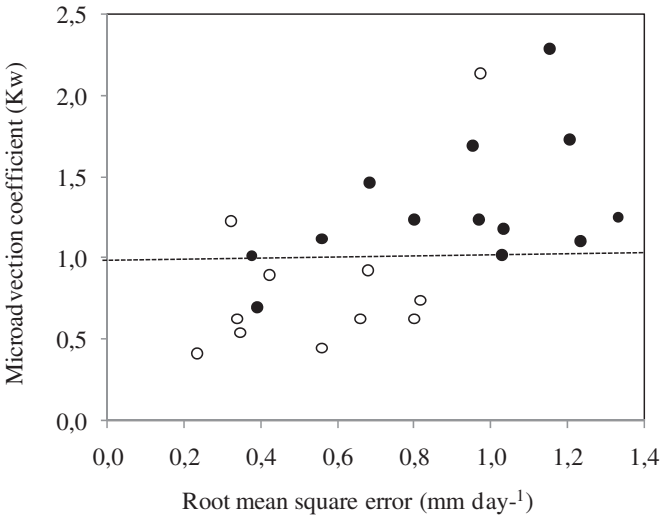

Fig. 7. The microadvection coefficient (K_w) as a function of the root mean square error (RMSE) between observed and estimated E_s. The means were obtained for each experimental period in sunlit and shaded areas, and for both moderate and high irrigation regimes. The black symbols correspond to the first day after irrigation and the white symbols to subsequent days after irrigation (>1 day).

increased with K_w for the first day after irrigation, while RMSE for subsequent days did not. These results indicate that an unbalance was present due to microadvection on the first day after irrigation, while the sum of vertical fluxes was balanced for the subsequent days. Lastly, there is a linear relationship between the average difference of the estimated (E_{sest}) and observed E_s values versus K_w for the shaded area on the first day after irrigation ($E_{sest} - E_s = 1.3K_w - 1$; $r^2 = 0.72$). The occurrence of a high average difference in the E_s estimation at high K_w values is consistent with microadvection.

Evett's model could be used to estimate optimal soil water content in olive orchards by determining the values of soil evaporation at which there is no microadvection for different times of the year. This occurs when the ratio of observed to estimated E_s, versus the soil water content is approximately one (Figuerola et al., 2007).

4. Conclusion

Small scale soil evaporation within a mature, drip-irrigated olive orchard depended on variably interacting effects of the irrigation regime, the seasons, and the position relative to the tree canopy. In the shaded area of the tree row, radiation transmitted through the tree canopy affected evaporation and besides evaporation is proportional to the soil surface area wetted by the drip emitters. While, vapor pressure deficit near the soil surface largely controlled the rate of evaporation in sunlit areas between trees in the crop row.

In our non-Mediterranean climate without winter precipitation and low summer rainfall, an irrigation experiment was carried out under a moderate and high regime of irrigation throughout the year. Microadvection occurred along the year in the high irrigation regime, while microadvection was observed only in the winter months under moderate irrigation. We did not observe the occurrence of microadvection in sunlit areas between trees in the crop row, but this was observed in shaded areas beneath the canopy. In May and August (end of autumn and winter) and particularly in the moderate irrigation regime, evaporation resulting in the shaded area was greater than in the sunlit area.

Analysis of the vertical temperature gradient near the soil surface was also consistent with microadvection. A downward sensible heat flux in the warmer months increased the latent heat flux to a

greater extent in the shaded area than in the sunlit area under the tree canopy for the first day after irrigation. Further analysis indicated microadvection during the daylight hours in the cooler months. Convective cells within the tree canopy may also result in the injection of sensible heat into the crop from the tree inter-row space.

Estimation of evaporation from a model that takes into account the energy balance resulted in an underestimate of the values observed in the first days after irrigation. This is due to the effect of microadvection in the area wetted by the emitters. The observed values for subsequent days after irrigation (>1 day) coincide with estimated evaporation and microadvection did not occur.

Acknowledgments

We thank Alan Fillmore for use of the commercial orchard "Anjullon B". The research was partially funded by the Agencia Nacional de Promoción Científica y Tecnológica de Argentina (PICT 2005 #32218, PICT 2007 #389).

References

Allen, R.G., Pereira, L.S., Raes, D., Smith, M., 1998. Crop evapotranspiration: guidelines for computing crop water requirements. In: FAO Irrigation and Drainage Paper No. 56. FAO, Rome.

Ayerza, R., Sibbett, G.S., 2001. Thermal adaptability of olive (*Olea europaea* L.) to the Arid Chaco of Argentina. Agriculture. Ecosystems and Environment 84, 277–285.

Ben-Asher, J., Matthias, A.D., Warrick, A.W., 1983. Assessment of evaporation from bare soil by infrared thermometry. Soil Science Society of America Journal 47, 185–191.

Berliner, P., 1998. Contribution of Heat Dissipated at the Soil Surface to the Energy Balance of a Citrus Orchard. Ph. D. thesis. Hebrew University, p. 111.

Bonachela, S., Orgaz, F., Villalobos, F.J., Fereres, E., 1999. Measurement and simulation of evaporation from soil in olive orchards. Irrigation Science 18, 205–211.

Bonachela, S., Orgaz, F., Villalobos, F.J., Fereres, E., 2001. Soil evaporation from drip irrigated olive orchards. Irrigation Science 20, 65–71.

Brutsaert, W.H., 1982. Evaporation into the Atmosphere. D. Reidel Publishing Company, Dordrecht, Holland.

Cohen, S., 1983. Light Relations in an Orchard. Ph. D. thesis. Hebrew University of Jerusalem, Israel.

Cooper, P.J., Keatinge, J.D.H., Hughes, G., 1983. Crop evapotranspiration – a technique for calculation of its components by field measurements. Field Crops Research 7, 299–312.

Cooper, P.J.M., Gregory, P.J., 1987. Soil water management in the rain-fed farming systems of the Mediterranean region. Soil Use and Management 3, 57–62.

Correa-Tedesco, G., Rousseaux, M.C., Searles, P.S., 2010. Plant growth and yield responses in olive (*Olea europaea*) to different irrigation levels in an arid region of Argentina. Agricultural Water Management 97, 1829–1837.

Diaz-Espejo, A., Verhoef, A., Knight, R., 2005. Illustration of micro-scale advection using grid-pattern mini-lysimeters. Agricultural and Forest Meteorology 129, 39–52.

Eastham, J., Gregory, P.J., Williamson, D.R., Watson, G.D., 1999. The influence of early sowing of wheat and lupin crops on evapotranspiration and evaporation from the soil surface in a Mediterranean climate. Agricultural Water Management 42, 205–218.

Eastham, J., Gregory, P.J., 2000. Deriving empirical models of evaporation from soil beneath crops in a Mediterranean climate using microlysimetry. Australian Journal of Agricultural Research 51, 1017–1022.

Evett, S.R., Matthias, A.D., Warrick, A.W., 1994. Energy balance model of spatially variable evaporation from bare soil. Soil Science Society of America Journal 58, 1604–1611.

Figuerola, P.I., Berliner, P., 2006. Characteristics of the surface layer above a row crop in the presence of local advection. Atmósfera 19, 75–108.

Figuerola, P.I., Searles, P., Rousseaux, M.C., 2007. A method to evaluate evaporation in olive orchard. Ciência e Natura, 125–128. Edição Especial – Micrometeorologia.

Fox, M.J., 1968. A technique to determine evaporation from dry stream beds. Journal of Applied Meteorology 7 (4), 697–701.

Gómez del Campo, M., Morales-Sillero, A., Vita Serman, F., Rousseaux, M.C., Searles, P.S., 2010. Olive growing in the arid valleys of Northwest Argentina (provinces of Catamarca, La Rioja and San Juan). Olivae 114, 23–45.

Kailis, S.G., Harris, D.J., 2007. Producing Table Olives. Landlinks Press, Collingwood VIC3066, Australia, p. 328.

Kreith, F., Sellers, W.D., 1975. General principles of natural evaporation. In: de Vries, D.A., Afgan, N.H. (Eds.), Heat and Mass Transfer in the Biosphere, Part1. John Wiley & Sons, New York, pp. 207–227.

Lang, A.R.G., Evans, G.N., Ho, P.Y., 1974. The influence of local advection on evapotranspiration from irrigated rice in a semi-arid region. Agricultural Meteorology 13, 5–13.

Lascano, R.J., Van Bavel, C.H.M., Hatfield, J.L., Upchurch, D.R., 1987. Energy and water balance of a sparse crop: simulated and measured soil and crop evaporation. Soil Science Society of America Journal 51, 1113–1121.

Lee, X., Yu, Q., Sun, X., Liu, J., Min, Q., Liu, Y., Zhang, X., 2004. Micrometeorological fluxes under the influence of regional and local advection: a revisit. Agricultural and Forest Meteorology 122, 111–124.

Mariscal, M.J., 1998. Intercepción de radiación solar y acumulación de biomasa por cubiertas de olivo. Doctoral thesis. University of Córdoba, Spain.

McNaughton, K.G., Laubach, J., 1998. Unsteadiness as a cause of non-equality of eddy diffusivities for heat and vapor at the base of an advective inversion. Boundary-Layer Meteorology 88, 479–504.

Orgaz, F., Testi, E.L., Villalobos, F.J., Fereres, E., 2006. Water requirements of olive orchards–II: determination of crop coefficients for irrigation scheduling. Irrigation Science 24, 77–84.

Perry, C., Steduto, P., Allen, R.G., Burt, C.M., 2009. Increasing productivity in irrigated agriculture: agronomic constraints and hydrological realities. Agricultural Water Management 96, 1517–1524.

Raupach, M.R., 1979. Anomalies in flux-gradient relationships over forest. Boundary-Layer Meteorology 16, 467–486.

Ritchie, J.T., 1972. Model for predicting evaporation from a row crop with incomplete cover. Water Resource Research 8, 1204–1213.

Rousseaux, M.C., Figuerola, P.I., Corea-Tedesco, G., Searles, P.S., 2009. Seasonal variations in sap flow and soil evaporation in an olive (*Olea europaea* L.) grove under two irrigation regimes in an arid region of Argentina. Agricultural Water Management 96, 1037–1044.

Rousseaux, M.C., Benedetti, J.P., Searles, P.S., 2008. Leaf-level responses of olive trees (*Olea europaea*) to the suspension of irrigation during the winter in an arid region of Argentina. Scientia Horticulturae 115, 135–141.

Tennant, D., Hall, D., 2001. Improving water use of annual crops and pastures – limitations and opportunities in Western Australia. Australian Journal of Agricultural Research 52, 171–182.

Testi, L., Villalobos, F.J., Orgaz, F., Fereres, E., 2006. Water requirements of olive orchards: I simulation of daily evapotranspiration for scenario analysis. Irrigation Science 24, 69–76.